International Information and Engineering Technology Association
Advancing the World of Information and Engineering

Annales de Chimie - Science des Matériaux
Vol. 45, No. 1, February, 2021, pp. 69-74
Journal homepage: http://iieta.org/journals/acsm

Effect of Martensite Morphologies on Corrosion in 5% H_2SO_4 Solution of Borided X70 Dual Phase Steel

Tassi Hocine, Zidelmel Sami*, Allaoui Omar

Laboratory Process Engineering, University of Laghouat, B.P. 37G route de Ghardaia, Laghouat 03000, Algeria

Corresponding Author Email: s.zidelmel@lagh-univ.dz

https://doi.org/10.18280/acsm.450109

Received: 12 November 2020
Accepted: 9 January 2021

Keywords:
dual phase steel, intercritical annealing, boronizing, corrosion properties

ABSTRACT

In the present investigation, some electrochemical properties of dual phase X70 steels with different martensite morphologies which have undergone boriding were studied. To obtain a variety of martensite morphologies, Direct Quenching (DQ), Intermediate Quenching (IQ) and Step Quenching (SQ) heat treatments were applied at an intercritical annealing temperature (IAT) of 760°C. The treatment (DQ) allowed the formation of fine martensite evenly distributed in the ferrite matrix. (IQ) treatment showed the formation of martensite along the ferrite / ferrite grain boundaries. In contrast, treatment (SQ) induced the formation of a banded morphology of martensite and ferrite. The realization of borides on X70 (DP) steel was carried out in a powder mixture containing 5% of B_4C as source of boron, 5% of $NaBF_4$ as activator and 90% of SiC as diluent at 950°C for a period of time from 4 h. The corrosion behavior of X70 (DP) steel has been explored by the Tafel extrapolation method in a 5 wt. % H_2SO_4 solution. The corrosion resistance of steel which has undergone boriding (BDP) is higher than that of steel which has not undergone it (DP).

1. INTRODUCTION

The Dual-phase (DP) steels belong to the High Strength Low Alloy (HSLA) class steels [1]. These steels have a mixture of ferritic (soft and ductile) and martensitic (hard and brittle) microstructures. In the search for the development of this microstructure, numerous heat treatments in the phase region ($\alpha + \gamma$) were carried out followed by rapid cooling [2, 3]. DP steels exhibit unique mechanical characteristics including good combination of high strength and formability. These mechanical properties make DP steels attractive for many applications [4-6]. For the same intercritical annealing conditions, the microstructure (DP) can have several morphologies. The morphology of martensite directly controls the mechanical properties of ferrite–martensite (DP) steels [7-9]. In addition to their incomparable combination of mechanical properties, the corrosion resistance of DP steels is critically important for structural and constructional purposes. A major problem usually limits the applications of pipeline steels in industry, where it suffers corrosion when exposed to aggressive media such as chloride containing and acid solutions. The corrosion of pipeline steels represents a big issue due to the high cost and time spending in replacing, repairing and maintaining the corroded parts [10, 11].

Although a lot of researches have been conducted, further investigation should be done on the effect various morphology between ferrite and martensite of (DP) steels to mechanical properties and corrosion behavior. The corrosion of (DP) steels has been reported by Bhagavathi et al. [12, 13] showing that the microstructure and test conditions directly affect the corrosion resistance of dual-phase steel. Investigations on the effect of corrosion behavior to the dual phase microstructure have been done by Trejo et al. [14], and Zhang et al. [15]. From their studies, they found that, dual phase microstructure has a good corrosion resistance. Osario et al. [16] have also studied electrochemical corrosion behaviour of low carbon steel in three different heat treated and as-received conditions by carrying out electrochemical impedance spectroscopy (EIS) and polarization test. Bhagavathi et al. [17] have recently reported that DP steels are more resistant to corrosion than the ferrite-pearlite steel.

Boronizing is a thermochemical treatment which consists in enriching the surface of the steel with boron in order to form boride layers at high temperatures. Boriding is hopeful thermochemical surface hardening treatment applied in several fields of engineering in order to improv their resistance to wear, oxidation and corrosion [18-20]. Currently, multiple boriding processes are available for the treatment of ferrous materials [21]. The powder boriding technique consists of conditioning the cleaned parts in a mixture of boronizing powder (source of boron+ dulient + activators) by heating it for a few hours depending on the desired thickness of the boride layer [22, 23]. The powder boriding process has important advantages: easy handling, the ability to change the composition of the powder, minimal equipment and the resulting cost savings. In this study, the solid boriding treatment was preferred because it is easy to apply, less expensive and has better properties. Boride layer on steels had exhibited good corrosion resistance against different acids HCl, H_2SO_4, HNO_3 and H_3PO_4 [17]. Yusuf Kayali [24] has study the electrochemical corrosion behaviors in a 3.5 wt.% NaCl solution of boronized dual-phase steel. They found that the formation of the boride layers improved the corrosion resistance of dual-phase steel up to 3 times. The corrosion behavior of pack produced boride layer of American Petrolium Institute (API) X70 Steel have not been examined extensively.

In this study Boriding of dual phase X70 steel by pack boriding was studied for which the boriding conditions (temperature and time) were fixed. In addition, the corrosion resistance of the layers developed under optimal conditions was monitored in a 5% solution of H_2SO_4. The corrosion data was obtained by electrochemical linear polarization techniques. The corrosion resistance of dual phase samples before (DP) and after (BDP) boriding were compared.

2. MATERIALS AND EXPERIMENTAL METHODS

The Commercial API X70 steel, whose chemical composition is given in Table 1, was used as initial material. The steel was supplied by Alpha pipe gaz society Ghardaia, Algeria. In order to obtain various morphologies of martensite, three types of heat treatment were applied at an intercritical annealing temperature (IAT) of 760°C, as shown in (Figure 1). The IQ treatment consisted of a double treatment: the samples were first heated at 940°C for 30 min and cooled with water, followed by heating at an intercritical temperature of 760°C for 30 min and quenched at the water. The IQ treatment consisted of directly heating the samples to an intercritical temperature of 760°C for 30 minutes followed by rapid cooling with water. In the SQ treatment, samples were first heated at 940°C for 30 min, cooled in the oven to the intercritical annealing temperature (IAT) of 760°C, held for 30 min and quenched in the water.

Boronizing was done in a powder mixture having 5 % B4C as boron source, 5% NaBF4 as activator and 90% SiC as dilluent. The boronizing was performed at 950°C and 4 h. The boride thickness measurement was carried out using a digital instrument integrated into the SEM microscope. Corrosion experiments were carried out at 25°C in a 5 wt. % H_2SO_4 solution. Potentiodynamic polarization experiments were carried out using a Potentiostat (Radiometer model PGZ 301). A conventional three-electrode cell was used for all the electrochemical measurements.

A saturated calomel electrode and a platinum electrode were used as reference electrodes and counter electrodes, respectively. A sample of X70 steel welded to copper wire and coated with resin was used as the working electrode.

The technique of linear polarization resistance allows estimating the corrosion rate. The polarization curves were obtained at a potential range of -800 to -100 mV at a scan step of 1 mV s^{-1}.

Table 1. Chemical composition of X70 steel

Elements	C	Mn	Si	S	Al	Nb	V	Ti	Fe
Mass %	0.07	1.52	0.043	0.039	0.035	0.045	0.048	0.003	Balance

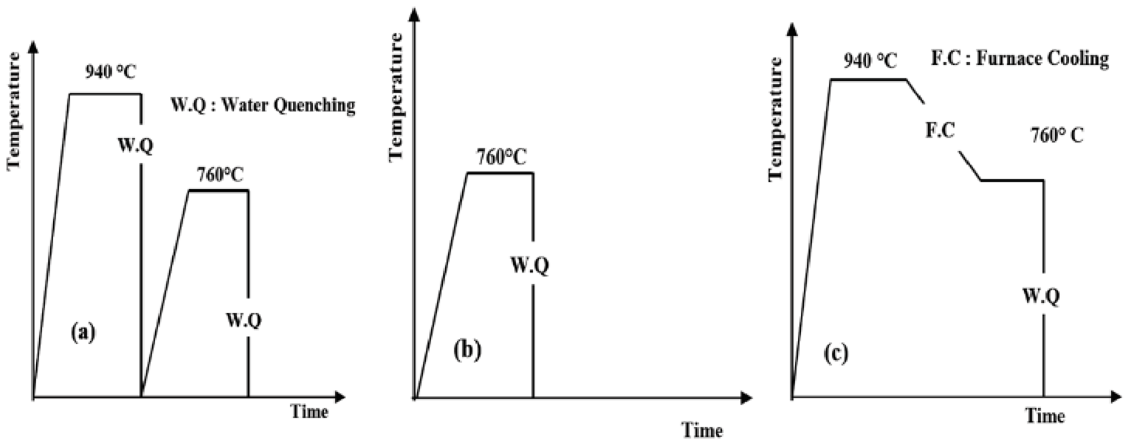

Figure 1. Schematic representation of heat treatment schedules for (a) IQ (b) DQ (c) SQ treatments

3. RESULTS AND DISCUSSION

3.1 Microstructures and mechanical properties

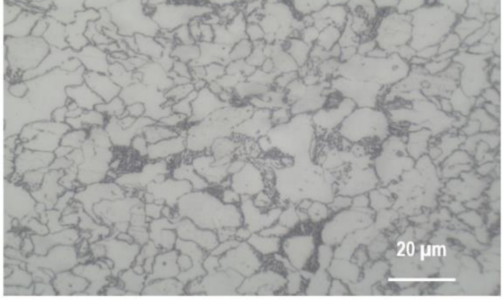

Figure 2. Ferrite / perlite microstructure of X70 steel as received

The microstructure (ferrite + perlite) of our steel in the initial state is shown in Figure 2. The ferrite which represents the matrix (light zone) and the pearlite occupies the grain boundaries.

Figure 3 shows the optical micrographs of X70 samples with different martensite morphologies subjected to different type of heat treatment treated at an intercritical annealing temperature (IAT) = 760°C.

It is clear that the treatments carried out give microstructures (DP); except that the shape, size and distribution of the martensitic phase vary considerably with the type of heat treatment. The (IQ) specimen indicates the microstructure with lath- type morphology of martensite distributing uniformly in the ferrite matrix (Figure 3a), the microstructure of (DQ) specimen showed polygonal ferrite surrounded by a connected network morphology of martensite along the ferritic grain boundaries (Figure 3b), whereas the ferrite and martensite in (SQ) specimen exhibited banded microstructures with blocky regions of the phases (Figure 3c). The change in the morphology of martensite was attributed to the difference in the initial microstructural state of the samples before reaching the intercritical domain ($\alpha + \gamma$) [1]. In IQ treatment, during heating to intercritical temperatures ($\alpha + \gamma$), the germination of austenite, from the initial totally martensitic microstructure, begins at the austenite grain boundaries the carbides and also at the joints of martensite slats thus forming regions acicular shaped and then transforms fine particles of martensite upon quenching at room temperature. The good dispersion of the germination sites favors the appearance of a martensite of fine and fibrous morphology uniformly dispersed in the final dual-phase microstructure [25, 26]. When the initial structure (ferrite + perlite) is warmed in the intercritical domain, the austenite germinates inside the perlite colonies and on the junctions of perlite colonies. During this time, austenite germinates on the ferrite-ferrite grain boundaries. Subsequently, this austenite turns into islands of martensite after quenching [27, 28].

In the case of the SQ treatment, the initial phase before annealing in the two-phase domain is the austenite phase. According to Thompson & Howell, the band structure appears after relatively slow cooling from the austenitic domain [29]. After cooling in the oven to temperatures in the ($\alpha + \gamma$) range, the ferrite germinates at the grain boundaries of the austenite and develops inside the austenite grains, which results in having two distinct regions of ferrite and austenite [30, 31].

The martensite volume fractions (MVF) obtained under (IQ), (DQ) and (SQ) treatments were quantified at 35%, for the annealing temperatures of 760°C. The martensite content depends on the intercritical temperature (ICT) and not on the various intercritical heat treatments, as it has been reported by some studies [1, 32]. The percentage volume fraction of martensite in dual phase steel is influenced by variation in the intercritical annealing temperature. The higher intercritical annealing temperature, the higher the percentage of the volume fraction of martensite in dual phase steel obtained. According to the Iron-Carbon diagram, as the intercritical annealing temperature increases, more austenite is transformed. The latter will then be transformed into martensite by rapid cooling while keeping the same proportion.

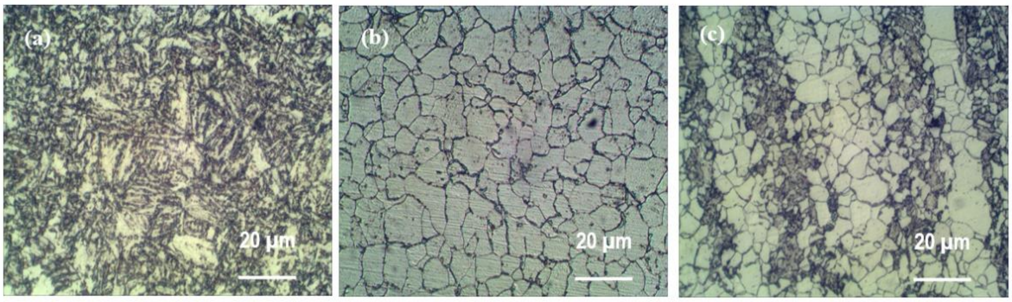

Figure 3. Optical micrographs of (a) IQT, (b) DQT and (c) SQT treatments at IAT=760°C showing ferrite (white) and martensite (black)

3.2 Boronized structure

Figure 4 shows SEM cross-sectional examinations of the borided X70 (BDP) steel with different heat treatment schedule (SQ, DQ and IQ) and uncloaked that the borides formed on the surface of the substrate have a saw tooth shape. The characteristics of the boride layer depend on the boride source used, boriding temperature, treatment time, and properties of the borided steel [33]. The obtained results showed that there was a formation of boride layers for all martensite morphologies for the boriding treatment at 950°C for 4 hours. However, it should be noted for all the treatments that the boride layers formed on the surface of the (DP) X70 steel may be single phase, consisting of the di-iron boride (Fe_2B). This morphology is a characteristics property of the boride layer in steels and depends on the boronizing source used, the boronizing temperature, the treatment time, and the properties of the boronized steel [34, 35]. During boriding, the diffusion and subsequent absorption of boron atoms through the matrix is controlled by the temperature and duration of the process. In addition, the chemical composition of steel is another important parameter and plays a major role in the diffusion of boron [36, 37].

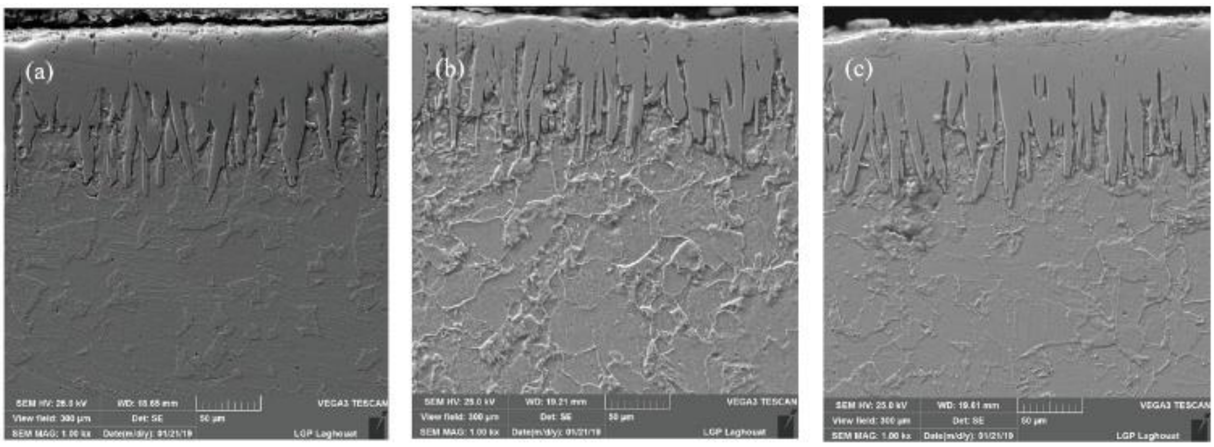

Figure 4. Micrograph of boride layer (a) DQT, (b) SQT and (c) IQT treatments

A layer of boride type (Fe_2B) is generally preferable for industrial applications, due to the difference between the specific volume and the coefficient of thermal expansion of the formed borides and the substrate [20, 21]. The formation of Fe_2B layers with a sawtooth morphology is desirable in the boriding of ferrous materials. The FeB phase is considered undesirable because FeB is more brittle than the Fe_2B layer. [33, 38]

3.3 Corrosion properties

The polarization curves of API X70 dual-phase steels with various martensite morphologies in 5 % H_2SO_4 solution are given in (Figure 5.a). Results of corrosion polarization studies of the X70 DP steel are grouped in Table 2. From the results, the lowest corrosion rate is 6.36 mm/yr which is from (SQ) specimen followed by (DQ) and (IQ) specimens which the corrosion rates are 7.687 mm/yr and 9.27 mm/yr respectively. Finally, the highest corrosion rate is 9.67 mm/yr for ferrite + Pearlite (FP) specimen. The corrosion resistance is better for all DP steels compared to (FP) sample steel. The rate of corrosion decreases as the microstructure changes from ferrite-perlite to ferrite-martensite. The following results can be clarified in the following way. The change from the initial structure (ferrite + pearlite) to a dual phase structure (ferrite + martensite), allowed the reduction of the galvanic couple between the phases. Figure 6 shows the structure (ferrite + pearlite) of X70 steel after corrosion in a 5% H_2SO_4 solution. It indicates that the perlite indicated by (P) is more resistant to corrosion, unlike ferrite (F) which degrades more.

It has been indicated that the ferrite acts as an anode in the galvanic couple of the ferrite + perlite structure [11, 22]. It was observed that the corrosion rate was found to depend on the morphologies of martensite phase in a 5 wt. % H_2SO_4 solution. At exception the IQ sample who owns a corrosion rate close to that of the FP sample, the other DP samples possess better corrosion properties than (FP) sample. However, present study shows that (DQ) treatment exhibited better corrosion properties than IQ treatment as expressed by its lower corrosion rate. The results of the present study conclude that the corrosion rate of steels (DP) with a ferrite-martensite structure is directly related to the morphology and the proportion of the phase constituents. The corrosion resistance of boronized (BFP) and (BDP) steels in a 5 wt. % H_2SO_4 solution was examined by polarization curves as shown in (Figure 5b). The results of the polarization corrosion study of DP X70 steel which underwent boronizing are shown in Table 2.

The corrosion resistance of the steel which has undergone boriding (BDP) is better, the value (Icorr) is lower and therefore the corrosion rate is lower compared to steels (DP) whatever the structure (BSQ- SQ, BDQ-DQ and BIQ -IQ). As can be seen from these results, the boriding process enhances the corrosion resistance of steels (DP).

From the results, the lowest corrosion rate is 0.311 mm/yr which is from BSQ specimen followed by BDQ and BIQ specimens which the corrosion rates are 0.355 mm/yr and 0.408 mm/yr respectively. All (BDP) samples exhibited a corrosion rate lower than that of (BPF) samples.

It was observed that the corrosion rates of all (BDP) steels were found to depend on the morphologies of martensite phase in a 5wt. % H_2SO_4 solution. It is known that the main aim of boriding is improving the corrosion resistance of steels. We have noticed that the boriding of the dual phase steels whatever the morphology of martensite, the resistance to corrosion is improved from 20 to 22 times.

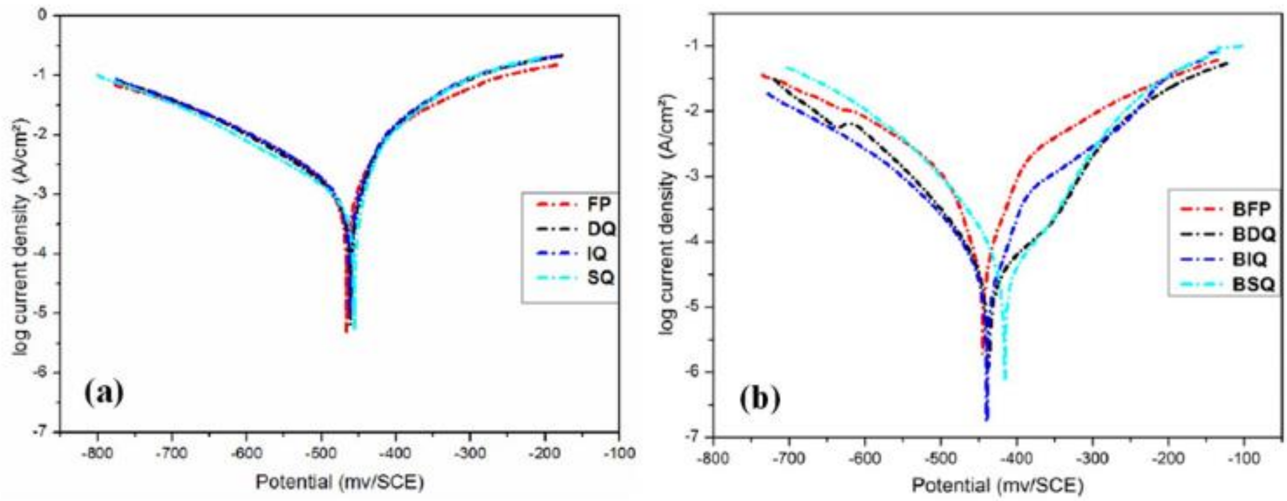

Figure 5. Tafel curves of (a) non-boronized and (b) boronized dual-phase steel at T=760°C

Table 2. Summary of result obtained from corrosion tests of (BDP) and (DP) steels performed in 5% H_2SO_4 solution

		DQ	SQ	IQ	FP
Before boriding	I_{corr} (mA/cm^2)	0.6573	0.5438	0.7926	0.8274
	corrosion rate (mm/Y)	7.687	6.360	9.27	9.677
	E (I=0) (mV)	-460.8	-455.6	-461.8	-465.9
After boriding	I_{corr} (mA/cm^2)	0.0303	0.0266	0.0349	0.0375
	corrosion rate (mm/Y)	0.355	0.311	0.408	0.438
	E (I=0) (mV)	-437.3	-416.7	-440.2	-445.4

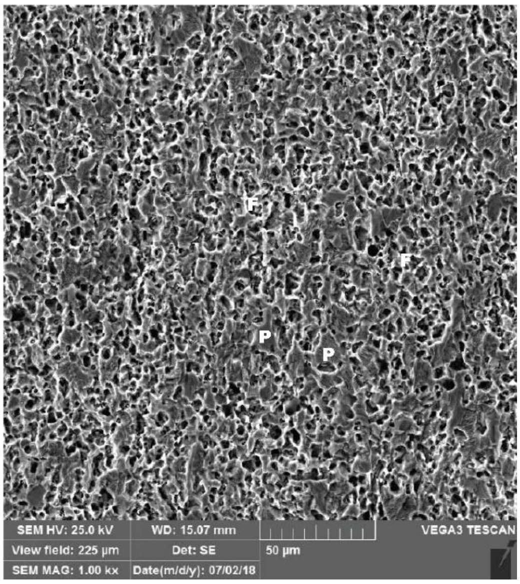

Figure 6. SEM micrograph of corroded Ferrite / perlite microstructure of X70 steel after potentiodynamic polarization in 5% H_2SO_4 solution

4. CONCLUSIONS

The corrosion of dual phase X70 pipeline steel with different morphologies of martensite in 5% H_2SO_4 solution before and after boriding has been reported. The study was performed using a potentiodynamic polarization.

Using the different IQ, DQ and SQ thermal processes at temperature 760℃ for 30 minutes, dual-phase microstructures with a variety of martensite morphologies were produced. The difference in the initial microstructural state of the samples before reaching the intercritical domain ($\alpha + \gamma$) can be held responsible for the differences observed in the morphology and distribution of martensite. It has been found that the variation in the morphology of martensite directly affects the corrosion resistance by varying the corrosion current, and the corrosion rate as indicated by polarization measurements. Boriding powder technique used at a temperature of 950℃ for 5 hours, allowed us to obtain a single layer of Fe2B type with sawtooth morphology. The boriding process improved the corrosion resistance of two-phase steel by 20 to 22 times compared to steel that did not undergo boriding.

ACKNOWLEDGMENTS

The authors gratefully acknowledge the financial support of the Directorate General for Scientific Research and Technological Development (DGRSDT).

REFERENCES

[1] Ahmad, E., Manzoor, T., Ziai, M.M.A. (2011). Effect of martensite morphology on tensile deformation of dual-phase steel. Journal of Materials Engineering and Performance, 21: 1-6. https://doi.org/10.1007/s11665-011-9934-z

[2] Erdogan, M. (2003). Effect of austenite dispersion on phase transformation in dual phase steel. Scripta Materialia, 48(5): 501-506. https://doi.org/10.1016/S1359-6462(02)00500-6

[3] Maleque, M.A., Poon, Y.M., Masjuki, H.H. (2004). The effect of intercritical heat treatment on the mechanical properties of AISI 3115 steel. Journal of Materials Processing Technology, 153-154: 482-487. https://doi.org/10.1016/j.jmatprotec.2004.04.391

[4] Masato, N., Nubuo, N. (2014). Effect of the martensite distribution on the strain hardening and ductile fracture behaviors in dual-phase steel. Materials Science and Engineering A, 604: 135-141. https://doi.org/10.1016/j.msea.2014.02.058

[5] Gunduz, S. (2009). Effect of chemical composition, martensite volume fraction and tempering on tensile behaviour of dual phase steels. Materials Letters, 63(27): 2381-2383. https://doi.org/10.1016/j.matlet.2009.08.015

[6] Zidelmel, S., Allaoui, O., Laidi, O., Benchatti, A. (2017). Influence of the heat treatments on martensite microstructure and abrasive wear behavior of X52 dual-phase steel. Modelling, Measurement and Control B, 86(3): 582-592. https://doi.org/10.18280/mmc_b.860301

[7] Saeidi, N., Ashrafizadeh, F., Niroumand, B. (2014). Development of a new ultrafine grained dual phase steel and examination of the effect of grain size on tensile deformation behaviour. Materials Science and Engineering A, 599: 145-149. https://doi:10.1016/j.msea.2014.01.053

[8] Seyedrezai, H., Pilkey, A.K., Boyd, J.D. (2014). Effect of pre-IC annealing treatments on the final microstructure and work hardening behavior of a dual-phase steel. Materials Science and Engineering A, 594: 178-188. https://doi.org/10.1016/j.msea.2013.11.034

[9] Bhagavathi, L.R., Banadkouki, S.S.G. (2014). Improvement of mechanical properties in a dual-phase ferrite–martensite AISI4140 steel under tough-strong ferrite formation. Materials and Design, 56: 232-240. https://doi.org/10.1016/j.matdes.2013.11.005

[10] Hegazy, M.A., Ahmed, H.M., El-Tabei, A.S. (2011). Investigation of the inhibitive effect of p-substituted 4-(N, N, N-dimethyldodecylammonium bromide) benzylidene-benzene-2-yl-amine on corrosion of carbon steel pipelines in acidic medium. Corrosion Science, 53(2): 671-678. https://doi.org/10.1016/j.corsci.2010.10.004

[11] Junaedi, S, Al-Amiery, A.A., Kadihum, A., Kadhum, A.A.H., Mohamad, A.B. (2013). Inhibition effects of a synthesized novel 4-aminoantipyrine derivative on the corrosion of mild steel in hydrochloric acid solution together with quantum chemical studies. International Journal of Molecular Science, 14(6): 11915-11928. https://doi.org/10.3390/ijms140611915

[12] Bhagavathi, L.R., Chaudhari, G.P., Nath, S.K. (2011). Mechanical and corrosion behaviour of plain low carbon dual-phase steels. Materials Design, 32(1): 433-440. http://dx.doi.org/10.1016/j.matdes.2010.06.025

[13] Sarkar, P.P., Kumar, P., Mana, K.M. (2005). Microstructural influence on the electrochemical corrosion behaviour of dual-phase steels in 3.5% NaCl solution. Materials Letters, 59(19-20): 2488-2491. http://dx.doi.org/10.1016/j.matlet.2005.03.030

[14] Trejo, D., Monteiro, P., Thomas, G., Wang, X. (1994). Mechanical properties and corrosion susceptibility of dual-phase steel in concrete. Cement and Concrete Research, 24(7): 1245-1254.

https://doi.org/10.1016/0008-8846(94)90109-0
[15] Zhang, C., Cai, D., Liao, B. (2004). A study on the dual-phase treatment of weathering steel 09CuPCrNi. Materials Letters, 58(9): 1524-1529. https://doi.org/10.1016/j.matlet.2003.10.018
[16] Osorio, W.R., Peixoto, L.C., Garcia, L.R., Garcia, A. (2009). Electrochemical corrosion response of a low carbon heat treated steel in a NaCl solution. Materials and Corrosion, 60(10): 804-812. https://doi.org/10.1002/maco.200805181
[17] Bhagavathi, L.R., Chaudhari, G.P., Nath, S.K. (2011). Mechanical and corrosion behavior of plain low carbon dual-phase steels. Materials and Design, 32(1): 433-440. https://doi.org/10.1016/j.matdes.2010.06.025
[18] Kartal, G., Kahvecioglu, O., Timur, S. (2006). Investigating the morphology and corrosion behavior of electrochemically borided steel. Surface Coating and Technology, 200(11): 3590-3593. https://doi.org/10.1016/j.surfcoat.2005.02.210
[19] Ozbek, I., Sen, S., Ipek, M., Bindal, C., Zeytin, S., Üçışık, A.H. (2004). A mechanical aspect of borides formed on the AISI 440 ℃ stainless-steel. Vacuum, 73(3-4): 643-648. https://doi.org/10.1016/j.vacuum.2003.12.083
[20] Pertek, A., Kulka, M. (2013). Microstructure and properties of composite (B + C) diffusion layers on low-carbon steel. Journal of Materials Science, 38: 269-273. https://doi.org/10.1023/A:1021153229913
[21] Sinha, A.K. (1990). ASM Handbook Volume 4 - Heat Treating, Boriding (Boronizing) of Steels: 437-447.
[22] Ozdemir, O., Omar, M.A., Usta, M., Zeytin, S., Bindal, C., Ucisik, A.H. (2008). An investigation on boriding kinetics of AISI 316 stainless steel. Vacuum, 83(1): 175-179. https://doi.org/10.1016/j.vacuum.2008.03.026
[23] Spence, T.W., Makhlouf, M.M. (2005). Characterization of the operative mechanism in potassium fluoborate activated pack boriding of steels. Journal of Materials Processing Technology, 168(1): 127-136. https://doi.org/10.1016/j.jmatprotec.2004.10.015
[24] Kayali, Y., Anaturk, B. (2013). Investigation of electrochemical corrosion behavior in a 3.5 wt.% NaCl solution of boronized dual-phase steel. Materials Design, 46: 776-783. https://doi.org/10.1016/j.matdes.2012.11.040
[25] Bag, A., Ray, K.K., Dwarakadasa, E.S. (1999). Influence of martensite content and morphology on the toughness and fatigue behavior of high-martensite dual-phase steels. Metallurgical and Materials Transaction A, 30: 1193-1202. https://doi.org/10.1007/s11661-999-0269-4
[26] Ahmad, E., Manzoor, T., Ziai, M.M.A., Hussain, N. (2012). Effect of Martensite morphology on tensile deformation of dual-phase steel. Journal of Materials Engineering and Performance, 21: 382-387. https://doi.org/10.1007/s11665-011-9934-z
[27] Hu, Y., Zuo, X., Li, R., Zhang, Z. (2012). Effect of initial microstructures on the properties of Ferrite-Martensite Dual-Phase pipeline steels with Strain-Based design. Materials Research, 15(2): 317-322. https://doi.org/10.1590/S1516-14392012005000021
[28] Rudnizki, J., Böttger, B., Prahl, U., Bleck, W. (2011). Phase-field modeling of austenite formation from a ferrite plus pearlite microstructure during annealing of cold-rolled dual-phase steel. Metallurgical and Materials Transactions A, 42: 2516-2525. http://dx.doi.org/10.1007/s11661-011-062
[29] Thompson, S.W., Howell, P.R. (1992). Factors influencing ferrite/pearlite banding and origin of large pearlite nodules in a hypoeutectoid plate steel. Materials Science and Technology, 8(9): 777-784. https://doi.org/10.1179/mst.1992.8.9.777
[30] Krebs, B., Germain, L., Hazotte, A., Goune, M. (2011). Banded structure in Dual Phase steels in relation with the austenite-to-ferrite transformation mechanisms. Journal of Materials Science, 46: 7026-7038. https://doi.org/10.1007/s10853-011-5671-9
[31] Erdogan, M. (2002). The effect of new ferrite content on the tensile fracture behaviour of dual phase steels. Journal of Materials Science, 37: 3623-3630. http://dx.doi.org/10.1023/A:10165489225
[32] Shi, L., Yan, Z., Liu, Y., Zhang, C., Qiao, Z. (2014). Improved toughness and ductility in ferrite/acicular ferrite dual-phase steel through intercritical heat treatment. Materials Science and Engineering A, 590: 7-15. https://doi.org/10.1016/j.msea.2013.10.006
[33] Allaoui, O., Bouaouadja, N., Saindernan, G. (2006). Characterization of boronized layers on a XC38 steel. Surface Coating and Technology, 201(6): 3475-3482. https://doi.org/10.1016/j.surfcoat.2006.07.238
[34] Meric, C., Sahin, S., Yilmaz, S.S. (2000). Investigation of the effect on boride layer of powder particle size used in boronizing with solid boron-yielding substances. Material Research Bulletin, 35(13): 2165-2172. https://doi.org/10.1016/S0025-5408(00)00427-X
[35] Sen, S., Sen, U., Bindal, C. (2005). The growth kinetics of borides formed on boronized AISI 4140 steel. Vacuum, 77(2): 195-202. https://doi-org.sndl1.arn.dz/10.1016/j.vacuum.2004.09.005
[36] Badini, C., Gianoglio, C., Pradelli, G. (1987). The effect of carbon, chromium and nickel on the hardness of borided layers. Surface and Coatings Technology, 30(2): 157-170. https://doi.org/10.1016/0257-8972(87)90140-X
[37] Carbucicchio, M., Palombarini, G. (1987). Effects of alloying elements on the growth of iron boride coating. Journal of Materials Science Letters, 6: 1147-1149. https://doi.org/10.1007/BF01729165
[38] Keddam, M., Chentouf, S.M. (2005). A diffusion model for describing the bilayer growth (FeB/Fe2B) during the iron powder-pack boronizing. Applied Surface Science, 252(2): 393-399. https://doi.org/10.1016/j.apsusc.2005.01.016